

## Giant cell-rich osteosarcoma in long bones: clinical, radiological and pathological features

### *Osteosarcoma ricco in cellule giganti delle ossa lunghe: caratteristiche cliniche, radiologiche e patologiche*

Cheng-Sheng Wang<sup>1,2</sup> • Qi-Hua Yin<sup>1</sup> • Jin-Sheng Liao<sup>1</sup> • Jiang-Hua Lou<sup>1</sup> • Xiao-Yi Ding<sup>1</sup>  
Yan-Bo Zhu<sup>3</sup>

<sup>1</sup>Department of Radiology, Ruijin Hospital, Shanghai Jiao Tong University School of Medicine, No.197, Ruijin 2nd Road, Shanghai 200025, China

<sup>2</sup>Department of Radiology, Union Hospital, Fujian Medical University, No. 29, Xinquan Road, Fuzhou 350001, China

<sup>3</sup>Department of Pathology, Ruijin Hospital, Shanghai Jiao Tong University School of Medicine, Shanghai, China  
Correspondence to: Xiao-Yi Ding, Tel.: +86-18-918967155, Fax: +86-21-64150737, e-mail: dxyrj@hotmail.com

Received: 17 February 2012 / Accepted: 26 March 2012 / Published online: 27 May 2013

© Springer-Verlag 2013

#### Abstract

**Purpose.** The purpose of this study was to review the clinical presentation, imaging, pathology and outcome of patients with giant cell-rich osteosarcoma (GCRO) of long bones.

**Materials and methods.** Radiography (n=9), magnetic resonance imaging (MRI) (n=6), computed tomography (CT) (n=3) and clinical course of nine patients (five males and four females; mean age, 26 years) with pathologically confirmed GCRO were retrospectively reviewed. Specific imaging findings, including size, eccentricity, ossification, lysis, cystic change, expansile growth, periosteal reaction, cortical destruction, soft tissue extension and joint involvement were documented.

**Results.** Presenting symptoms were pain in six patients and pain and palpable mass in three. An ill-defined margin surrounding a predominantly osteolytic lesion was detected at the proximal tibia (n=7) or femur (n=2) on imaging studies. Seven cases showed limited ossification. Three cases had tumours in the metaphysis and six in the metaepiphysis. The average maximum tumour dimension was 4.7 cm×5.2 cm×7.8 cm. Microscopically, tumours were composed of atypical cells with scanty osteoid formation and multinucleated giant cells. All patients received chemotherapy, and surgery was performed in eight patients. Three patients were dead and six were alive at the last follow-up.

**Conclusions.** GCRO is a rarer variant that has very close resemblance to giant cell tumour. Patients usually present nonspecific symptoms of pain and palpable mass. It usually

#### Abstract

**Obiettivo.** Lo scopo di questo studio è stato di rivedere la presentazione clinica, le caratteristiche all'imaging, la patologia e gli esiti di pazienti con osteosarcoma ricco in cellule giganti delle ossa lunghe

**Materiali e metodi.** Radiografia (n=9), imaging con risonanza magnetica (MRI) (n=6), tomografia computerizzata (CT) (n=3) e decorso clinico di nove pazienti (cinque maschi e quattro femmine; età media 26 anni) con GCRO confermato anatomo-patologicamente sono stati esaminati retrospettivamente. Specifici rilievi di imaging, inclusi dimensione, eccentricità, ossificazione, lisi, evoluzione cistica, crescita espansiva, reazione periostale, distruzione corticale, estensione ai tessuti molli e coinvolgimento articolare sono stati documentati.

**Risultati.** I sintomi di presentazione sono stati il dolore in sei pazienti e sia il dolore che la massa palpabile in tre pazienti. All'imaging è stato riscontrato un margine indefinito che circonda una lesione prevalentemente osteolitica a livello della tibia prossimale (n=7) o del femore (n=2). Sette dei casi hanno mostrato ossificazione limitata. In 3 casi il tumore era localizzato alla metafisi ed in 6 nella meta-epifisi. La massima dimensione tumorale è stata in media di 4,7 cm×5,2 cm×7,8 cm. Microscopicamente, i tumori erano composti di cellule tumorali atipiche con scarsa formazione di osteoide e cellule giganti multinucleate. Tutti i pazienti hanno ricevuto chemioterapia e un intervento chirurgico è stato eseguito su 8 pazienti. Tre pazienti erano morti e 6 erano in vita all'ultimo follow-up.

shows an osteolytic lesion with locally spared new bone formation in the metaphysis and/or metaepiphysis on imaging. Histologically, the atypical tumour cells with osteoid formation and multinucleated giant cells are the key factor in the diagnosis and differential diagnosis.

**Keywords** Bone neoplasms · Giant cell tumour of bone · Osteosarcoma · Tomography · X-ray · Computed tomography · Magnetic resonance imaging

**Conclusioni.** GCRO è una variante più rara che assomiglia molto al tumore a cellule giganti. I pazienti di solito presentano sintomi aspecifici come dolore e massa palpabile. Di solito si dimostra una lesione osteolitica con neoformazione ossea localmente conservata nella metafisi e/o meta-epifisi all'imaging. Istologicamente, le cellule tumorali atipiche con formazione di osteoide e le cellule giganti multinucleate sono i fattori chiave nella diagnosi e nella diagnosi differenziale.

**Parole chiave** Neoplasia ossea · Tumore osseo a cellule giganti · Osteosarcoma · Tomografia computerizzata · Risonanza magnetica

## Introduction

Osteosarcoma is the most common nonhaemopoietic primary malignant tumour of bone and in which neoplastic cells produce osteoid [1]. For giant cell-rich osteosarcoma (GCRO), the multinucleated giant cells are so obvious that these cells cover up the heteromorphic tumour cells of osteosarcoma, and histological images of many uniformly distributed multinucleated osteoclast-like giant cells are similar to giant cell tumour of bone [2]. GCRO is the rare subtype of primary osteogenic sarcoma and was first reported by Bathurst et al. in 1986 [3]. It constitutes about 3% of all osteosarcomas [3, 4]. GCRO is usually misdiagnosed as giant cell tumour of bone, as they have similar radiological and pathological features, which have seldom been reported in the literature [3, 5–9]. Owing to the different prognoses and treatment strategies for these tumours, it is important to make the right diagnosis [8].

To the best of our knowledge, there is a paucity of literature regarding patients with GCRO. Only 18 cases have been reported in the literature to date (Table 1) [2–11]. The purpose of this study was to review clinical, radiological and pathological features of GCRO of long bones.

## Materials and methods

Nine consecutive patients admitted to the authors' institution between February 1997 and December 2011 were reviewed. There were five men and four women, with a mean age of 26 (median age, 19; range, 13–51) years. Workup included radiographs – available in all cases – magnetic resonance imaging (MRI) in six and computed tomography (CT) in three. Lung metastases were evaluated by CT scan. Information on follow-up was available for all nine patients. Follow-up after diagnosis ranged from 5 to 114 (average,

60) months. All patients except one (patient no. 9, who is still under preoperative chemotherapy) underwent surgical treatment. Three patients were dead, five were alive without disease and one was alive with disease at the last follow-up. Patient demographic information and clinical course are shown in Table 2.

Symptoms and their duration were related to the time of first hospital admission. Tumour size was assessed by measuring the largest size of the anteroposterior length, height and width on radiography. Final tumour size (centimetres) was expressed as the multiplication of three diameters. Histological criteria to define GCRO were as follows: on low-power view, these lesions show multinucleated giant cells simulating a giant cell tumour; on high power, cytological anaplasia of stromal cells and malignant osteoid production can be identified [5, 11, 12].

In the initial radiological diagnosis, six patients were diagnosed as having giant cell tumour; one patient each was diagnosed with malignant tumour, possible osteosarcoma and osteosarcoma. In the initial pathological diagnosis, six patients were diagnosed as having GCRO and three with giant cell tumour. Detailed diagnostic results are shown in Table 3.

## Results

### Clinical findings

Presenting symptoms were pain duration for <3 months in three patients and between 3 and 6 months in three. Two patients had pain for 1 year, and one had pain for 2 years. Three patients complained of both pain and palpable mass. Average symptom duration was 7 (range 2–24) months (Table 4).

**Table 1** Previously reported 18 cases of giant cell-rich osteosarcoma**Tabella 1** Diciotto casi riportati precedentemente di osteosarcoma ricco in cellule giganti

Author	Age/sex	Symptoms	Location	Radiological findings	Recurrence and metastasis	Follow-up
Bathurst et al [3]	41/F	Pain and palpable mass	Femur diaphysis	Expansile lytic lesion with ill defined margins, the cortex is breached with a soft-tissue mass	Local recurrence, lung	DWD, 3 years
	13/F	Pain and palpable mass	Tibia diaphysis	Lytic lesion with periosteal reaction	None	NED, 16 years
	21/M	Tender palpable mass in thigh	Femur diaphysis	Ill-defined, expansile lytic with periosteal reaction	Local recurrence	NED, 9 years
	12/M	Ache, ununited fracture	Femur diaphysis	Expansile lytic with pathological fracture	Sacrum	DWD, 3 years
	6/F	Pain and limping	Tibia metaphysis	Lytic, slightly expansile lesion with pathological fracture	None	NED, 7 years
	16/F	Pain above knee	Femur diaphysis	Lytic, slightly expansile, ill defined lesion with periosteal reaction, pathological fracture	Recurrence, lung	DWD, 2 years
	12/M	Palpable mass and dysfunction	Tibia metaphysis	Ill-defined, expansile lytic lesion	Recurrence, lung	DWD, 2 years
	20/M	Pain in knee	Femur condyle	Ill-defined, expansile lytic lesion	None	NED, 2 years
	8/M	Palpable mass in thigh; limp	Femur diaphysis	Mixed sclerotic and lytic lesion with Codman's triangle, soft tissue mass and pathological fracture	None	NED, 1 year
Sato et al [10]	19/M	Motion pain	Femur metadiaphysis	Osteolytic lesion, cortical thinning and ballooning, onion skin-like periosteal reaction	None	NED, 6 years
Bertoni et al [5]	19/M	Fracture	Femur diaphysis	Osteolytic lesion with wide geographic margins, cortical destruction, soft tissue extension	Recurrence, multiple bone metastasis	DWD, 20 years
Shinozaki et al [6]	17/M	Pain, palpable mass, local heat, tenderness	Distal radius	Osteolytic lesion	Recurrence, multiple bone metastasis, lung	DWD, 41 months
Hong et al [7]	29/F	Pain	Tibia metaphysis	Osteolytic lesion, well-margined mass with cortical destruction and small soft tissue	None	NED, 11 months
Nagata et al [8]	32/M	Pain and palpable mass	Distal femur	Ill-defined, centric expansile lytic lesion with pathological fracture	None	NED, 20 months
Kinoshita et al [9]	16/M	Pain	11th rib	Eccentric hemispherical osteolytic lesion with disappearance of the cortex, Codman's triangle-like periosteal reaction	None	NED, 5 years
Fu et al [2]	67/F	Progressive growth of painless mass	Mandible	Osteolytic lesion	None	NED, 1 year
Verma et al [4]	56/F	Cheek palpable mass, nasal obstruction and nasal discharge	Maxilla	Expansile, hyperdense soft tissue mass, areas of calcification within the substance of tumour with sclerosis of adjacent bone	None	NED, unknown
Gambarotti et al [11]	29/M	Pain	Femur metadiaphysis	Osteolytic lesion	Recurrence	NED, unknown

DWD, dead with disease; NED, no evidence of disease; M, male; F, female

**Table 2** Basic information and clinical course of giant cell-rich osteosarcoma*Tabella 2* Informazioni di base e decorso clinico dell'osteosarcoma ricco in cellule giganti

Patient no.	Age/sex	Location	Treatment	Recurrence and metastasis	Follow-up/outcome
1	51/M	Proximal femur	Chemotherapy, local excision with prosthesis for initial management; amputation for local recurrence	Local recurrence, lung	DWD, 18 months
2	18/M	Proximal tibia	Amputation and chemotherapy	None	NED, 92 months
3	36/F	Proximal tibia	Curettage and cement filling for initial management; amputation and chemotherapy for local recurrence	Local recurrence	NED, 90 months
4	13/M	Proximal tibia	Curettage and allograft bone implantation for initial management; chemotherapy for local recurrence and pulmonary metastases	Local recurrence, lung	DWD, 13 months
5	19/F	Distal femur	Amputation and chemotherapy	None	NED, 74 months
6	33/F	Proximal tibia	Curettage and allograft bone implantation after interoperative frozen section; amputation and chemotherapy after paraffin section	None	NED, 111 months
7	16/M	Proximal tibia	Amputation and postoperative chemotherapy	Lung	DWD, 20 months
8	15/F	Proximal tibia	Amputation and chemotherapy	None	NED, 114 months
9	32/M	Proximal tibia	Preoperative chemotherapy	$\frac{3}{4}$	Alive with disease, 5 months

DWD, dead with disease; NED, no evidence of disease; M, male; F, female

## Imaging findings

Seven osteosarcomas were in the proximal tibia, one in the proximal femur and one in the distal femur. Three patients had tumours in the metaphysis and six in both the metaphysis and epiphysis, of which four were predominantly in the metaphysis and two in the epiphysis. Specific imaging findings, including size, eccentricity, ossification, lysis, cystic change, expansile growth, periosteal reaction, cortical destruction, soft tissue extension and joint involvement, are summarised in Table 4.

Radiographically, all tumours appeared as geographic osteolytic lesions with ill-defined margins (Figs. 1, 2). The average maximum tumour dimension was 4.7 cm×5.2 cm×7.8 cm (range: 3–7 cm×3–7 cm×4–12 cm). Cortical destruction and soft tissue extension were detected in three patients (Fig. 2). A Codman triangle or onion-skin-like periosteal reaction was observed in the lateral side of the tibia in two patients (Fig. 2). There was detectable new bone formation in four patients (Figs. 1, 2). Six lesions were eccentric and three were centric. There was an impending fracture of the medial cortex in one patient (Fig. 1). In brief, radiographic findings of lysis were seen in nine patients; eccentric growth in six; ossification in four; expansile growth, cortical destruction and soft tissue extension in three; periosteal reaction and joint involvement in two.

Three patients underwent CT scanning that clearly showed a large area of low-attenuated mass with focal bone formation. All lesions were eccentric. The cortex was thinned, with partial destruction and slight ballooning. Two lesions extended into the medullary cavity, resulting in a subtle fracture with minimal displacement. All lesions were osteolytic, with an incomplete thin rim of cortical bone through which soft tissue extension could be seen (Fig. 3). Two lesions destroyed the articular surface and involved the knee joint (Fig. 3d,e). After intravenous administration of contrast agent, diffuse strong enhancement was seen in the mass, except in the necrotic area (Fig. 3c–e). Summarising, CT features of eccentricity, ossification, lysis, cortical destruction and soft tissue extension were showed in three patients, expansile growth and joint involvement in two and periosteal reaction in one.

MR scanning was performed in six cases, of which five lesions were eccentric and one was centric. Five lesions were lobulated, ill-defined, isointense masses except for a focal area of low signal intensity compared with the signal intensity of skeletal muscle on T1-weighted images (Figs. 4a,b and 5a,b); diffuse heterogeneous high signal intensities with focal low signal intensity areas (suggestive of new bone formation) were evident on T2-weighted (Figs. 4c and 5c) and short-tau inversion recovery (STIR) images (Fig. 4d). There were different degrees of long T1 and long T2 concentrated or scattered areas of necrosis, and no evidence

**Table 3** Initial radiological and pathological diagnosis of giant cell-rich osteosarcoma**Tabella 3** Diagnosi iniziale radiologica e patologica dell'osteosarcoma ricco in cellule giganti

Patient no.	Initial radiological diagnosis	Initial pathological diagnosis
1	Giant cell tumour	Giant cell-rich osteosarcoma
2	Malignant tumour	Giant cell-rich osteosarcoma
3	Giant cell tumour	Giant cell tumour
4	Giant cell tumour	Giant cell tumour
5	Possible osteosarcoma	Giant cell-rich osteosarcoma
6	Giant cell tumour	Giant cell tumour
7	Osteosarcoma	Giant cell-rich osteosarcoma
8	Giant cell tumour	Giant cell-rich osteosarcoma
9	Giant cell tumour	Giant cell-rich osteosarcoma



**Fig. 1a,b** A 16-year-old boy with GCRO in the metaphysis of the tibia (patient no. 7). **a** Radiograph showing eccentric geographic osteolytic lesion with impending fracture in the medial cortex. **b** There was detectable new bone formation in the anterior aspect.

**Fig. 1a,b** Ragazzo di 16 anni con GCRO nella metafisi tibiale (paziente n° 7). **a** La radiografia mostra una lesione osteolitica eccentrica con frattura nella corticale mediale **b** Sul versante anteriore è visibile la neoproduzione di tessuto osseo.

of focal fluid–fluid level was noted (Fig. 5a–c). One lesion showed homogeneous low signal intensity on T1-weighted images and mixed high signal intensity on T2-weighted and STIR images. After intravenous administration of contrast material, diffuse or lace-like strong enhancement was seen in the masses, except for the necrotic portion and areas of new bone formation (Figs. 4e, f and 5d–f). Three eccentric lesions in the proximal tibias destroyed focal cortices and articular surfaces and involved the knee joints, through which small soft tissue extensions were observed (Fig. 4b–d, f). On the whole, MRI features, regarding lysis, were displayed in six patients: eccentricity, ossification and cystic change in five, cortical destruction and soft tissue extension in four, joint involvement in three and expansile growth in one.

#### Pathological features

All tumours were composed of atypical tumour cells and

osteoid formation in the final multispot sampling. Lesions showed multinucleated giant cells simulating a giant cell tumour (Fig. 6a). The scanty, coral-like, lacy, lamellar and cordal osteoid formation was arranged among the cytologic anaplasia of the stromal cells (Fig. 6b). The tumour cells had slightly basophilic cytoplasm, which showed a wide variety of morphologies such as round, oval, spindle-shaped, short spindle and polygonal. Heteromorphism of tumour cells was obvious. Many uniformly distributed multinucleated osteoclast-like giant cells could be seen among the tumour cells (Fig. 6c). Heteromorphism of giant cells was not obvious with pallid-stained cytoplasm.

#### Discussion

As subtypes of conventional osteosarcoma, GCRO and other subtypes are listed separately as unusual histological

**Table 4** Clinical features and imaging findings of giant cell-rich osteosarcoma

**Tabella 4** Caratteristiche cliniche e riscontri all'imaging dell'osteosarcoma ricco in cellule giganti

Patient no.	Symptoms	Symptom duration (months)	Size (cm)	Eccentricity	Ossification	Lysis	Cystic change	Expansile growth	Periosteal reaction	Cortical destruction	Soft tissue extension	Joint involvement
1	Pain	2	4x4x11	-	+	+	-	-	-	-	-	-
2	Pain	2	7x7x11	+	+	+	-	-	-	+	+	+
3	Pain, palpable mass	12	7x7x8	+	+	+	-	+	+	+	+	-
4	Pain	5	4x7x12	-	+	+	+	+	+	-	-	-
5	Pain	2	5x5x6	+	+	+	+	-	-	-	-	-
6	Vague pain, palpable mass	24	3x3x4	+	-	+	+	-	-	+	+	-
7	Pain, palpable mass after a fall	5	5x6x8	+	+	+	+	-	-	+	+	+
8	Pain	3	4x4x5	-	-	+	-	-	-	-	-	-
9	Paroxysmal pain	12	3x4x5	+	+	+	+	+	-	+	+	+

forms [1]. About 13–25% of cases of osteosarcoma, accompanied by a few osteoclast-like giant cells, can be seen in haemorrhagic and perivascular areas [13, 14], but the histology of GCRO with a large number of osteoclast-like giant cells similar to giant cell tumour is rare. Bathurst et al. [3] reported nine cases, accounting for 3% of osteosarcomas. In our collection of 305 cases of osteosarcoma, only nine cases presented the giant cell-tumour-like structure, accounting for 2.9%.

Mean age of all patients at diagnosis, including those in this study, was 24.7 (range 6–67) years. The patient group comprised 16 men and 11 women. This type of lesion tends to develop in a wide range of ages, with a male predominance (1.5:1). In all reported cases, including the cases in this study, 12 affected the femur, 11 the tibia and one each the radius, rib, mandible and maxilla, respectively. A large number of cases (n = 23) reside in the femur and tibia, where other conventional osteosarcomas and giant cell tumours are typically situated. Patients usually present non-specific clinical symptoms. The two most common chief complaints in these patients were pain (21 cases, 77.8%) and palpable mass (12 cases, 44.4%). The differential diagnosis of GCRO includes conventional osteosarcoma, giant cell-rich, malignant fibrous histiocytoma, as well as benign and malignant giant cell tumours. GCRO was distinguished from conventional osteosarcoma on the basis of the predominantly osteolytic lesion without notable ossification or periosteal reaction on imaging findings, and on histological findings of numerous giant cells with scanty osteoid. The basic proliferating component of giant cell-rich malignant fibrous histiocytoma is a fibrohistiocytic cell exhibiting a storiform or pinwheel pattern and never forming bone or osteoid directly [15, 16]. Also, the moth-eaten or permeative pattern of bone destruction seen on imaging findings was not compatible with recent cases [17]. The long bones are the predilection sites for both GCRO and giant cell tumour. However, the vast majority of GCROs are metaphyseal, whereas most giant cell tumours occur in the epiphysis. Primary involvement of the epiphysis is extraordinarily rare in osteosarcoma [18]. On imaging, a typical giant cell tumour of bone is the eccentric bubble-like osteolytic destruction without periosteal reaction. In histology, the key factor to differentiate the two is osteoid formation [2]. Except for osteoclast-like giant cells, heteromorphism and mitosis of tumour cells with more or less osteoid in GCRO can be seen, whereas many uniformly distributed osteoclast-like giant cells, interstitial oval or short spindle-shaped mononucleated cells without osteoid of tumour can be seen in giant cell tumour. GCRO should be differentiated from malignant giant cell tumour.

The radiographic appearances of malignant giant cell tumours are similar to those of benign giant cell tumours [19]. Microscopic examination reveals that direct formation

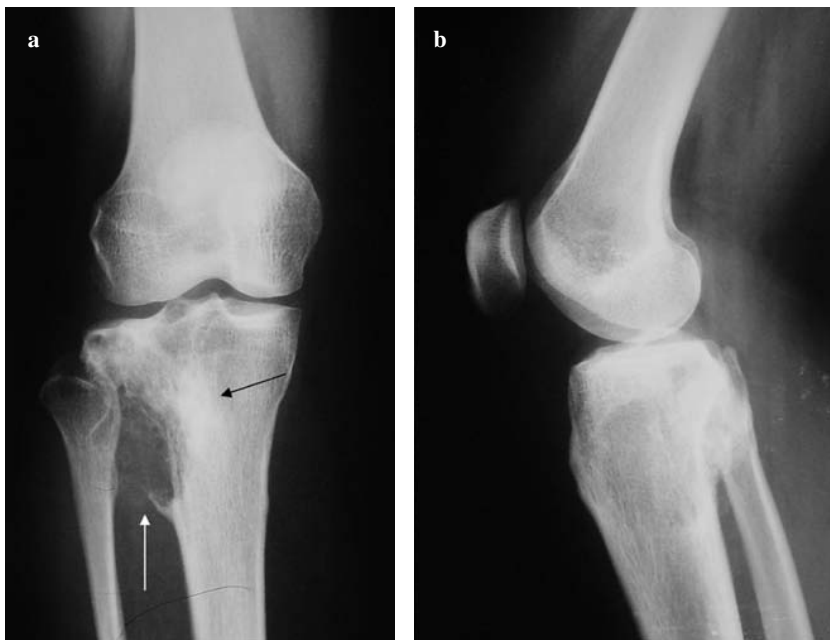


**Fig. 2a,b** A 36-year-old woman with GCRO in the proximal tibia (patient no. 3). **a** A Codman triangle of periosteal reaction with soft tissue extension is seen in the lateral cortex of the tibia (white arrow). There was detectable new bone formation medially (black arrow). **b** Ill-defined osteolytic bone destruction detected in the metaphysis.

**Fig. 2a,b** Donna di 36 anni con GCRO della tibia prossimale (paziente n° 3). **a** È visibile il triangolo di Codman da reazione periostale con estensione ai tessuti molli sul profilo corticale laterale della tibia (freccia bianca). Medialmente è individuabile la neoproduzione di tessuto osseo (freccia nera). **b** Nella metafisi è individuabile area di osteolisi a margini indefiniti.

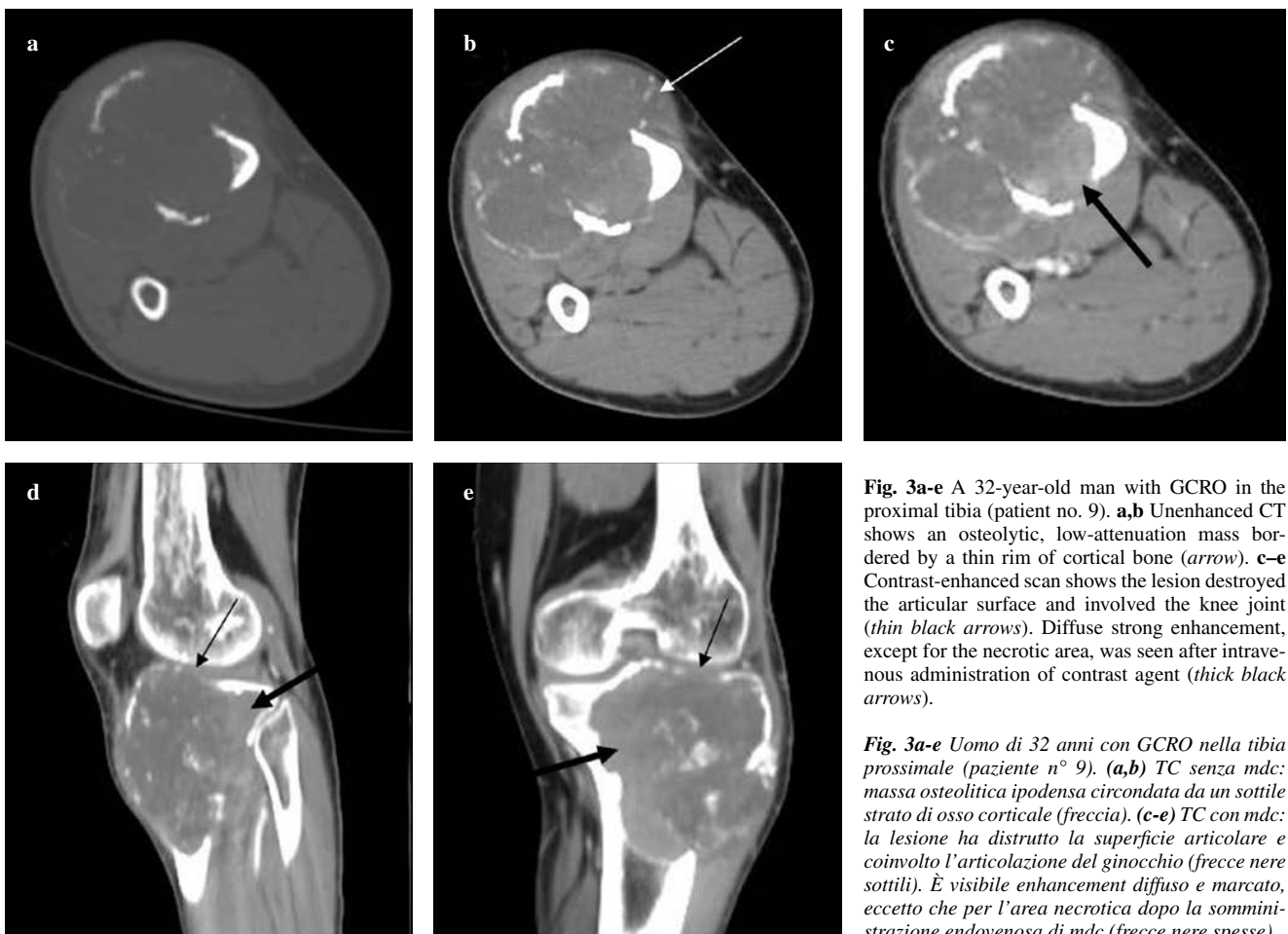


**Fig. 3a-e** A 32-year-old man with GCRO in the proximal tibia (patient no. 9). **a,b** Unenhanced CT shows an osteolytic, low-attenuation mass bordered by a thin rim of cortical bone (arrow). **c-e** Contrast-enhanced scan shows the lesion destroyed the articular surface and involved the knee joint (thin black arrows). Diffuse strong enhancement, except for the necrotic area, was seen after intravenous administration of contrast agent (thick black arrows).

**Fig. 3a-e** Uomo di 32 anni con GCRO nella tibia prossimale (paziente n° 9). **(a,b)** TC senza mdc: massa osteolitica ipodensa circondata da un sottile strato di osso corticale (freccia). **(c-e)** TC con mdc: la lesione ha distrutto la superficie articolare e coinvolto l'articolazione del ginocchio (freccie nere sottili). È visibile enhancement diffuso e marcato, eccetto che per l'area necrotica dopo la somministrazione endovenosa di mdc (freccie nere spesse).

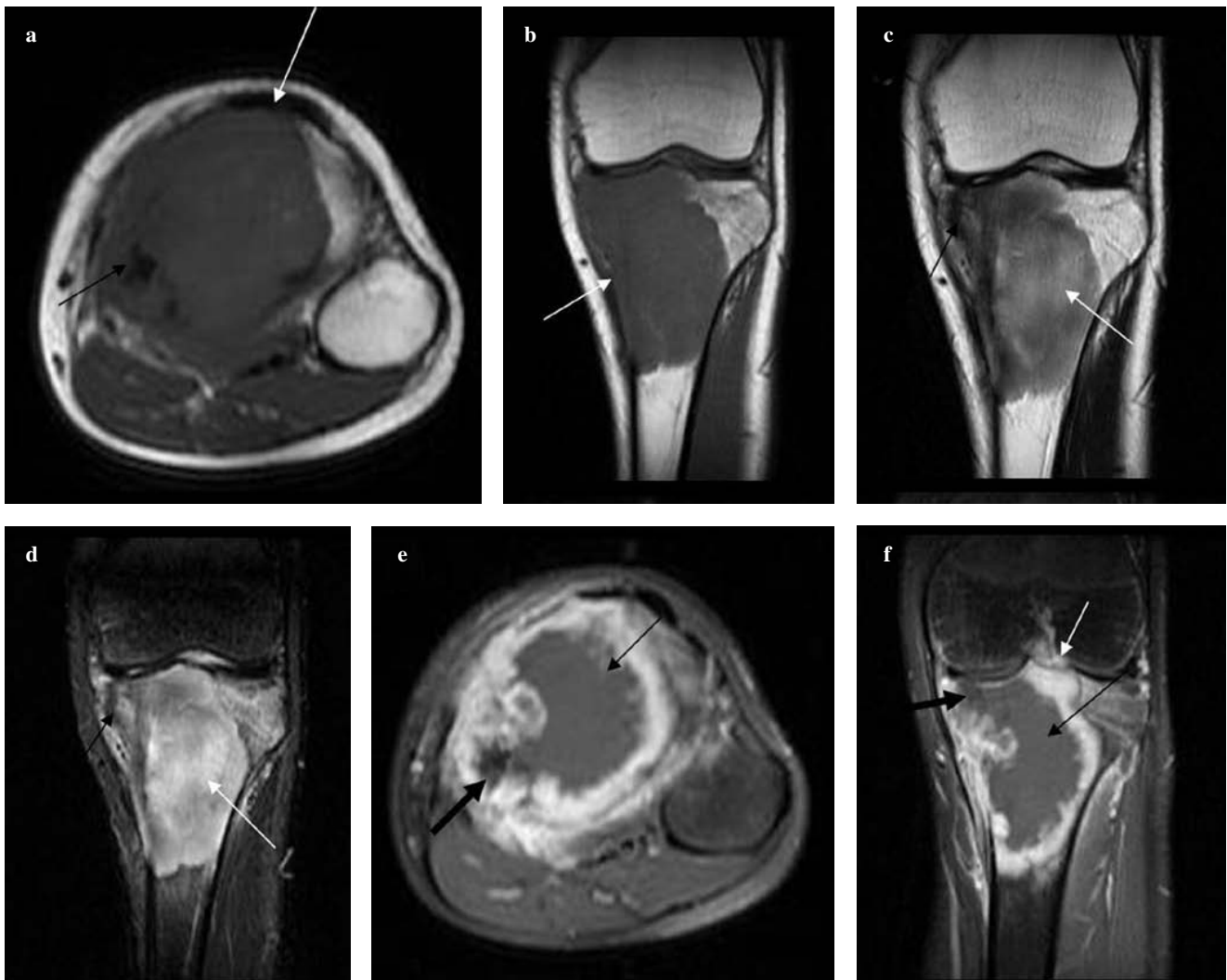


**Fig. 4a-f** An 18-year-old boy with GCRO in the proximal tibia (patient 2): **a,b** T1-weighted magnetic resonance (MR) image. Lesion was mostly isointense (white arrow) with focal low signal intensities (black arrow) compared with muscle. **c** T2-weighted image. **d** STIR images. The tumour showed heterogeneous high signal intensity (white arrow) containing focal low signal intensity (black arrow). **e,f** Fat-suppressed contrast-enhanced scans. Diffuse or lacelike strong enhancement was seen in the mass, except for the area of necrosis (thin black arrows) or bone formation (thick black arrows). The eccentric lesion destroyed the focal cortex and articular surface and involved the knee joints (white arrow).

**Fig. 4a-f** Ragazzo di 18 anni con GCRO nella tibia prossimale (paziente n° 2): **a,b** RM (immagine T1-pesata): la lesione ha prevalentemente segnale isointenso (freccia bianca) con focale ipointensità (freccia nera) rispetto al muscolo. **c,d** RM (immagine T2-pesata e immagine STIR): il tumore mostra segnale eterogeneo iperintenso (freccia bianca) contenente area di focale ipointensità (freccia nera). **e,f** RM (acquisizione con soppressione del grasso dopo mdc): intenso enhancement diffuso o cordoniforme nella massa tranne che nell'area di necrosi (freccie nere sottili) o di neoproduzione ossea (freccie nere spesse). La lesione eccentrica ha distrutto la corticale focale e la superficie articolare ed ha coinvolto le articolazioni del ginocchio (freccia bianca).

of osteoid by the malignant spindle cells is not seen in malignant giant cell tumours, and an area of giant cell tumour is present in addition to verified areas of sarcomatous stroma [20]. This may be the key factor in differentiating these two lesion types.

Radiological features of GCRO are different from those of conventional osteosarcoma. The diagnosis of GCRO is very difficult, as they mimic nonmineralised benign or malignant bone tumours [4]. Bathurst et al. [3] described the typical radiographic pattern of GCRO as an ill-defined mar-

gin surrounding a predominantly lytic lesion. They noted that a soft tissue mass is usually not present and the periosteal reaction is weak. In our study, five of the nine patients showed a soft tissue mass with different degrees of cortical destruction, which may be related with tumour size and eccentric growth. In addition, cross-sectional images are more specific than plain radiography in characterising a soft tissue mass. We also found that tumours in the epiphyses of proximal tibias were more likely to cause soft tissue extensions and destroy the knee joints, which may be related to



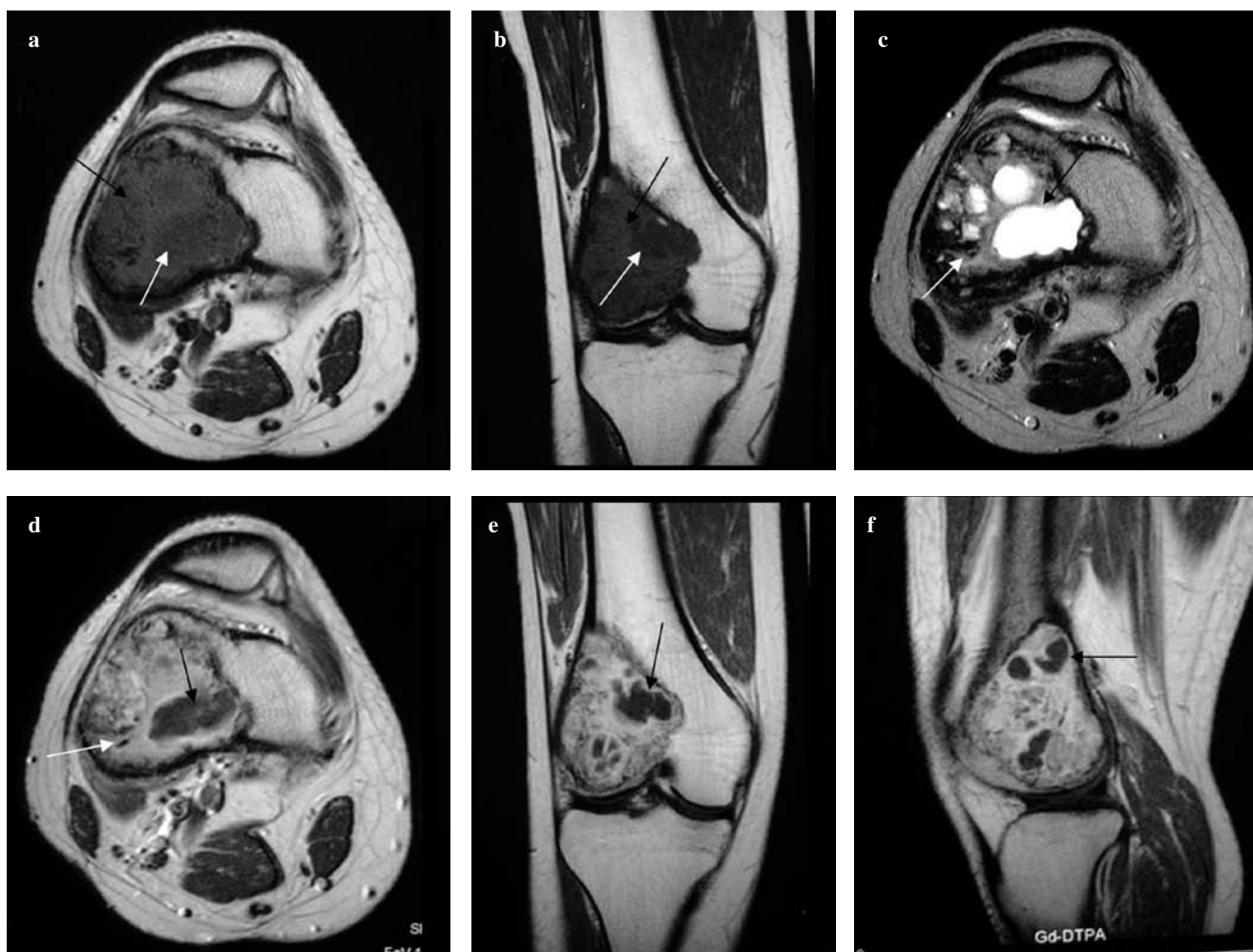


**Fig. 5a-f** A 19-year-old girl with GCRO in the distal femur (patient 5): **a,b** T1-weighted images. The lesion showed isointense signal (*black arrows*) with slightly lower signal intensities (*white arrows*). **c** T2-weighted image. The tumour showed diffuse heterogeneous high signal intensity (*black arrow*) with focal spotty areas of low signal intensity (*white arrow*). **d-f** Contrast-enhanced scan. Diffuse strong enhancement was seen in the major portion of the mass, except for the areas of necrosis (*black arrows*) and bone formation (*white arrow*).

**Fig. 5a-f** Ragazza di 19 anni con GCRO nel femore distale (paziente n° 5): **a,b** RM (immagine T1-pesata): la lesione mostra segnale isointenso (freccie nere) con aree con intensità di segnale leggermente inferiore (freccie bianche). **c** RM (immagine T2-pesata): il tumore mostra un segnale ad alta intensità diffuso ed eterogeneo (freccia nera) con aree focali di segnale ipointenso (freccia bianca). **d-f** RM con mdc: enhancement diffuso e marcato nella maggior parte della massa tumorale tranne che per le aree di necrosi (freccie nere) e di neoproduzione di tessuto osseo (freccia bianca).

the predominantly cancellous bone of the epiphyses. Local new bone formation is a typical appearance that shows a dense focus on radiograph and CT imaging, and low signal intensity on all MRI pulse sequences. On retrospective analysis in our study, seven patients showed locally spared new bone formation. The low detection rate in our study and the previous literature [3] with radiography may be related to overlapping images and limited ossification. CT and MRI can help assess the invasion of medullary or adjacent joint, new bone formation, destruction of cortex and soft tissue extension. In our study, due to lack of knowledge regarding the spectrum of GCROs and nonspecific osteolytic destruction with limited ossification on imaging, six patients were

misdiagnosed as having giant cell tumour at initial radiological diagnosis.

The histopathologic characteristics that identify GCRO include the presence of numerous osteoclast-like giant cells, with scanty osteoid formation by the tumour cells [4, 10, 11]: but osteoid formation in some GCROs was very limited, and heteromorphism of mononuclear tumour cells was not obvious. In addition, GCRO often creates difficulty in making a diagnosis when tissue samples do not include osteoid [2, 9]. Thus, the diagnosis of GCRO is challenging.

In this study, three cases were initially misdiagnosed as giant cell tumour. Tumour recurred in two cases after 3–5 months and was then diagnosed as GCROs. One case was

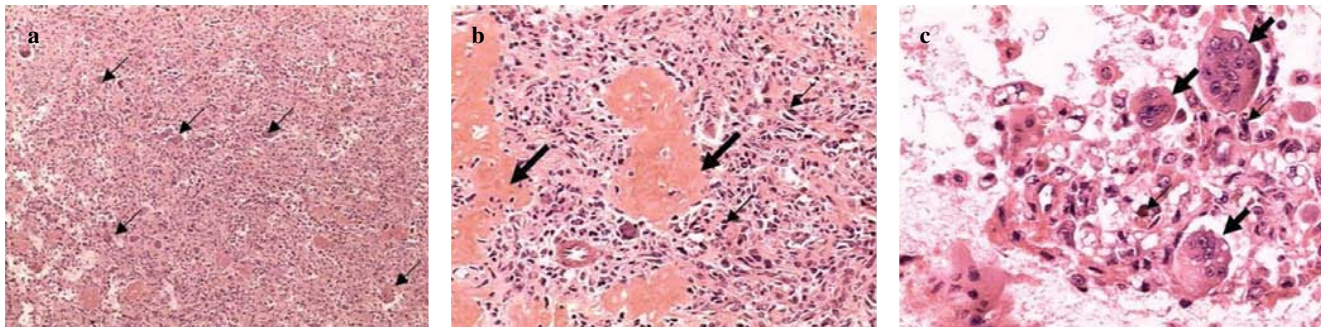


**Fig. 6a-c** GCRO: **a** lesion showed multinucleated giant cells (*arrows*) simulating a giant cell tumour [hematoxylin and eosin (H&E),  $\times 40$ ]. **b** Cytologic anaplasia of stromal cells (*thin arrows*) and malignant osteoid production (*thick arrows*) can be identified (H&E,  $\times 200$ ). **c** Numerous multinucleated osteoclast-like giant cells (*thick arrows*) can be seen among the round, oval, spindle-shaped, short spindle and polygonal atypical tumour cells (*thin arrows*) (H&E,  $\times 360$ ).

**Fig. 6a-c** Microfotografie di GCRO: **a** la lesione mostra cellule giganti multinucleate (*freccie*) che simulano un tumore a cellule giganti (ematossilina-eosina,  $40\times$ ). **b** Anaplasia citologica delle cellule stromali (*freccie sottili*) e produzione di osteoide di aspetto maligno (*freccie spesse*) (ematossilina-eosina,  $200\times$ ). **c** Numerose cellule giganti multinucleate osteoclasto-simili (*freccie spesse*) possono essere viste tra le cellule tumorali atipiche, rotonde, ovali, fusiformi, fusiformi brevi e poligonali (*freccie sottili*) (ematossilina-eosina,  $360\times$ ).

diagnosed as a giant cell tumour in interoperatively surgical frozen section, and paraffin-section review established a diagnosis of GCRO. Histological examination could only depict a small area, which may have complicated the diagnosis, especially as the tissue was drawn from the site of converted osteoclast-like giant cells with inconspicuous osteoid. Pathological tissues should be drawn from multiple sites, so heteromorphism and pathological mitosis of tumour cells should be observed carefully.

Poor prognostic indicators include the presence of metastasis and local recurrence. Of the 27 cases of GCRO diagnosed (Tables 1 and 2), nine developed metastasis and ten had local recurrence. Local recurrence is the most important factor influencing survival rate. Reportedly, the lung and bone are frequent sites of metastasis from GCRO [3, 5, 6]. Sites of distant metastasis included the lung (six cases), bone (two cases) and both lung and bone (one case). Of the nine patients (seven men, two women) who died, all died of metastatic disease 13 months to 20 years after diagnosis.

Male sex was identified as an indicator of poor outcome, which was compatible with conventional osteosarcoma [21]. The 5-year survival rate of 57.9% (11/19) was similar to the reported rate of 60–80% [22, 23]. These observations reflect the similar prognosis of GCRO, compared with conventional osteosarcoma.

## Conclusions

GCRO is a rarer variant of, and has very close resemblance to, giant cell tumour. Patients usually present nonspecific symptoms of pain and palpable mass. GCRO usually shows an osteolytic lesion, with locally spared new bone formation in the metaphysis and/or metaepiphysis on imaging. Histologically, atypical tumour cells with osteoid formation and multinucleated giant cells are the key factor in diagnosis and differential diagnosis. Prognosis is similar to that of conventional osteosarcoma.

**Acknowledgements** This study was supported by the National Natural Science Foundation of China (Project Number: 81072188).

**Conflict of interest** The authors declare that they have no conflict of interest related to the publication of this article.

## References/Bibliografia

1. Fletcher CDM, Unni KK, Mertens F (2002) World Health Organization Classification of Tumours. Pathology and genetics of tumours of soft tissue and bone. IARC Press, Lyon, pp 264–286
2. Fu HH, Zhuang QW, He J et al (2011) Giant cell-rich osteosarcoma or giant cell reparative granuloma of the mandible? *J Craniofac Surg* 22:1136–1139
3. Bathurst N, Sanerkin N, Watt I (1986) Osteoclast-rich osteosarcoma. *Br J Radiol* 59:667–673
4. Verma RK, Gupta G, Bal A, Yadav J (2011) Primary giant cell rich osteosarcoma of maxilla: an unusual case report. *J Oral Maxillofac Surg* 10:159–162
5. Bertoni F, Bacchini P, Staals EL (2003) Giant cell-rich osteosarcoma. *Orthopedics* 26:179–181

6. Shinozaki T, Fukuda T, Watanabe H, Takagishi K (2004) Giant cell-rich osteosarcoma simulating giant cell tumor of bone. *Kitakanto Med J* 54:147–151
7. Hong SJ, Kim KA, Yong HS et al (2005) Giant cell-rich osteosarcoma of bone. *Eur J Radiol Extra* 53:87–90
8. Nagata S, Nishimura H, Uchida M et al (2006) Giant cell-rich osteosarcoma of the distal femur: radiographic and magnetic resonance imaging findings. *Radiat Med* 24:228–232
9. Kinoshita G, Yasoshima H (2006) Giant cell-rich tumor of the rib. *J Orthop Sci* 11:312–317
10. Sato K, Yamamura S, Iwata H et al (1996) Giant cell-rich osteosarcoma: a case report. *Nagoya J Med Sci* 59:151–157
11. Gambarotti M, Donato M, Alberghini M, Vanel D (2011) A strange giant cell tumor. *Eur J Radiol* 77:3–5
12. Mirra JM (1989) Bone tumors: clinical, radiologic and pathologic correlation. Lea and Febiger, Philadelphia, pp 326–333
13. Unni KK (1988) Bone tumors. Churchill Livstone, New York, pp 117
14. Troup JB, Dahlin DC, Coventry MB (1960) The significance of giant cells in osteogenic sarcoma. Do they indicate a relationship between osteogenic sarcoma and giant cell tumor of bone. *Proc Staff Meet Mayo Clin* 35:179–186
15. Huvos AG, Heilweil M, Bretsky SS (1985) The pathology of malignant fibrous histiocytoma of bone. A study of 130 patients. *Am J Surg Pathol* 9:853–871
16. Ballance WA Jr, Mendelsohn G, Carter JR et al (1988) Osteogenic sarcoma. Malignant fibrous histiocytoma subtype. *Cancer* 62:763–771
17. Link TM, Haeussler MD, Poppek S et al (1998) Malignant fibrous histiocytoma of bone: conventional X-ray and MR imaging features. *Skeletal Radiol* 27:552–558
18. Raymond AK, Murphy GF, Rosenthal DI (1987) Case report 425: Chondroblastic osteosarcoma: clear-cell variant of femur. *Skeletal Radiol* 16:336–341
19. Bertoni F, Bacchini P, Staals EL (2003) Malignancy in giant cell tumor. *Skeletal Radiol* 32:143–146
20. Nascimento AG, Huvos AG, Marcove RC (1979) Primary malignant giant cell tumor of bone: a study of eight cases and review of the literature. *Cancer* 44:1393–1402
21. Janeway KA, Barkauskas DA, Krailo MD et al (2012) Outcome for adolescent and young adult patients with osteosarcoma: A report from the Children’s Oncology Group. *Cancer* 118:4597–4605; DOI: 10.1002/cncr.27414
22. Goorin AM, Abelson HT, Frei E 3rd (1985) Osteosarcoma: fifteen years later. *N Engl J Med* 313:1637–1643
23. Glasser DB, Lane JM, Huvos AG et al (1992) Survival, prognosis, and therapeutic response in osteogenic sarcoma. The Memorial Hospital experience. *Cancer* 69:698–708